Journal of Biomolecular Techniques
17:114–121 © 2006 ABRF

Metal Ion–Mediated Reduction in Surface Entropy Improves Diffraction Quality of Crystals of the IRAK-4 Death Domain

Michael V. Lasker,[1,2] Santosh M. Kuruvilla,[1] Mark M. Gajjar,[1] Anubhav Kapoor,[1] Satish K. Nair[1,3]

[1]Department of Biochemistry, [2]Medical Scholars Program, [3]Center for Biophysics and Computational Biology, University of Illinois at Urbana-Champaign, Urbana, IL

Interleukin-1 receptor–associated kinase-4 (IRAK-4) is an essential component of innate immunity in mice and humans. IRAK-4 is a bipartite protein composed of a death domain (DD) that mediates molecular recognition, and a catalytic kinase domain. Structure determination of the proteolytically stable, soluble IRAK-4 DD was hampered by poor diffraction quality. Addition of manganese (II) chloride to the crystallization solution produced significant improvements in diffraction, and the structure has been determined to 1.7-Å resolution. Examination of the IRAK-4 DD crystal structure reveals a single manganese ion coordinated to surface residues lysine-21 and aspartate-24. Coordination of the manganese ion resulted in a reduction in the surface entropy at this region of the molecule, by generating a contact-forming and conformationally homogenous surface patch. Prior studies have shown that surface entropy reduction by mutation of surface residues with large flexible side chains (i.e., Lys and Glu) to smaller side chains results in the production of diffraction-quality crystals. The intrinsic high surface entropy of Lys residues can also be decreased by reductive methylation. Our results suggest that screening of manganese ions as a crystallization additive may also facilitate ordered crystallization by reduction of surface entropy. Given the quick and inexpensive nature of screening, this technique is likely to be amenable to high-throughput methods such as those employed by Protein Structure Initiatives.

Key Words: X-ray crystallography, death domain, innate immunity, surface entropy, diffraction.

The immune system that mediates the cellular response is typically divided into two categories: (1) adaptive and (2) innate responses.[1] The adaptive response is induced following recovery of an infection from a pathogen. In contrast, the innate response is activated immediately upon infection. Innate immunity utilizes germline-encoded, broadly specific receptors to recognize highly conserved molecular structures, called *pathogen-associated molecular patterns*, found in many different microorganisms.[2] These molecular patterns can be specific to a particular type of pathogen, but are not found in the host. Lastly, the innate immune system does not retain a memory of prior exposure.[3] In vertebrates, the innate immune response regulates the release of mediators of inflammation, such as cytokines (tumor necrosis factor-alpha, interleukin-1, etc.) and chemokines (interleukin-8).[4]

Activation of the mammalian innate immune response pathway is initiated by the direct recognition of pathogen-associated molecular patterns by the extracellular domain of a member of the Toll-like receptor family.[5] Receptor activation results in the recruitment of a multi-protein signaling complex through interactions mediated by the cytoplasmic Toll/IL-1 receptor/resistance (TIR) domain of the Toll-like receptor and the TIR domain of the universal adaptor MyD88.[6] In turn, the MyD88 adaptor recruits downstream kinases, including the interleukin receptor–associated kinase-4 (IRAK-4).[7] This signaling cascade eventually culminates in the activation of NFκB and the production of proinflammatory cytokines. Given the role of the innate immune pathway in mediating inflammation,[8] there has been extensive research on the components of the innate immune pathway. However, there have been few studies to investigate the structural details of these components. As a step towards structural

Address correspondence and reprint requests to: Michael V. Lasker, Department of Biochemistry, University of Illinois at Urbana-Champaign, 600 South Mathews Avenue, Urbana, IL 61801 (phone: 217-333-2688; fax: 217-244-5858; email: lasker@uiuc.edu).

Present affiliations: University of Chicago, Chicago, Illinois (S.M.K. and M.M.G.)

characterization of key players within this pathway, we have determined the crystal structure of the death domain of IRAK-4.[9]

Initial crystallization screens identified promising conditions that were further refined to yield well-formed crystals. However, diffraction from these crystals was poor and was limited to a Bragg limit of 4 Å. Presumably, this weak diffraction was due to a high surface entropy introduced by either a dynamic tail, loop, or side chain. To reduce this surface entropy and subsequently produce crystals that had improved diffraction properties, we sought to identify a more stable protein construct by using limited proteolysis. Treatment of samples of the IRAK-4 death domain with various proteases demonstrated that the protein construct used for crystallization represented a stable core domain. Size-exclusion chromatography documented that the purified protein was monomeric and not prone to further aggregation. Screening of various additives yielded crystals grown in the presence of manganese chloride that showed a marked improvement in diffraction quality to a limiting resolution of 1.7 Å. The structure was solved by multiwavelength anomalous diffraction methods using a crystal transiently soaked in a high concentration of sodium bromide.[10] Inspection of the final structure shows that a single manganese ion generates a contact-forming and conformationally homogenous surface patch consisting of a Lys and an Asp residue. To our knowledge, this is the first time manganese ions have been shown to reduce surface entropy of proteins. We propose that the use of manganese ions to limit surface entropy may be a generally feasible means of improving diffraction qualities of protein crystals.

MATERIALS AND METHODS

Cloning and Expression

The cDNA of the *Mus musculus* IRAK-4 gene, mouse 30017484 pSPORT1, was purchased from the American Type Culture Collection (Manassas, VA). The polymerase chain reaction (PCR) using Pfx polymerase (Invitrogen, Carlsbad, CA) amplified the region corresponding to the death domain of IRAK-4, amino acids 1–113. PCR was carried out using the following primers (Integrated DNA Technologies, Coralville, IA): forward, 5'-CAGCAGCCGCATATGAACAAGCCGTTGACACC-3'; reverse, 5'-CCGCTCGAGTTACTAAGGCAGGCTTT-3', restriction enzyme recognition sites underlined. The amplified PCR product was purified using the Qiaquick PCR purification kit (Qiagen, Valencia, CA) and the fragment was digested with *NdeI* and *XhoI* (New England Biolabs, Ipswich, MA) overnight at 37°C. The digested PCR product was ligated into a modified pGEX6p1 vector (Amersham Biosciences, Piscataway, NJ) using T4 DNA ligase (Invitrogen). The ligation mixture was then used to transform chemically competent DH5α *E. coli* cells. Samples positive for insertion were then sent for dideoxy sequencing to confirm that the proper gene was cloned into the vector and that the insert was in frame. The resultant fusion plasmid produces the IRAK-4 death domain as a carboxy-terminal fusion with glutathione S-transferase (GST-IRAK4 DD).

The GST-IRAK4 DD vector was used to transform BL21 (DE3) *E. coli* chemically competent cells. An expression check was carried out by growing transformants 4 h in 2 mL of Luria broth (LB) containing 200 μg/mL ampicillin at 37°C. A small sample was removed and the remaining culture was induced using 1 mM (final concentration) isopropyl-β-D-thiogalactoside (IPTG). After 3 h at 30°C, 500 μL of both the induced and uninduced samples were pelleted by centrifugation, and the media were removed. The pellets were resuspended in 100 μL of H_2O by vortexing. Equal volumes of the resuspension and 2X sodium dodecyl sulfate (SDS) sample loading buffer were mixed, typically 15-μL volumes, heated at 95°C for 5 min, and loaded onto a 10% SDS–polyacrylamide gel electrophoresis (PAGE) gel for analysis.

For large-scale expression, a small-scale starter culture containing ampicillin (200 mg/L) was inoculated with single colonies of BL21 (DE3) bearing the GST-IRAK4 vector and incubated with vigorous shaking at 37°C. Approximately 5 h later, the starter cultures were used to inoculate 6 L of LB bearing the same concentration of ampicillin. This culture was then induced with a final concentration of 0.5 mM IPTG when the optical density at $\lambda = 600$ nm reached 0.6–0.8. Protein expression continued for 16–18 h at 18°C. The cells were harvested by centrifugation and resuspended using 20 mM HEPES (pH 7.5), 100 mM KCl, 10% glycerol, DNAase, and a protease inhibitor cocktail purchased from Sigma (St. Louis, MO). After resuspension, the cells were flash frozen in liquid nitrogen and stored at –80°C until needed.

Purification

Frozen cells were thawed and disrupted by multiple passes through an Avestion C5 French pressure cell. Following lysis, cellular debris was removed by centrifugation (15,000 rpm, 1 h). The supernatant was then applied to a glutathione sepharose (Amersham Pharmacia) column that had been equilibrated in 1X phosphate-buffered saline (PBS) (pH 7.4), 500 mM KCl, at a flow rate of 0.5 mL/min. The column was then washed at a flow rate of 2 mL/min for 150 min with the same equilibration buffer. The sample was then eluted using 20 mM reduced glutathione, 200 mM

Tris (pH 8.3), and 500 mM KCl. Fractions (10 mL) were then analyzed by SDS-PAGE. Fractions containing GST-IRAK-4 DD were then dialyzed in 20 mM MES (pH 6.5), 100 mM KCl (buffer A), using a 6000–8000 molecular-weight cutoff (MWCO) dialysis bag. Rhinoviral 3C protease (~100 μg) was added to the dialysis bag and the sample was then allowed to dialyze overnight at 4°C. The sample was then analyzed for protease cleavage by SDS-PAGE. Upon complete cleavage, the dialysate was loaded onto a HiTrap SP FF 5-mL column (Amersham Biosciences), previously equilibrated with buffer A, at a flow rate of 2 mL/min. After loading and washing with buffer A (~30 mL), a linear gradient to 1 M KCl over 24 column volumes was used to elute the untagged protein. The fractions were analyzed by SDS-PAGE to determine the fractions containing untagged IRAK-4 DD. Fractions containing IRAK-4 DD were pooled and stored in 10% (v/v) glycerol, aliquoted, flash frozen in liquid nitrogen, and stored at –80°C.

Size-Exclusion Chromatography

A Sephadex 75 (Amersham Biosciences) gel filtration column was equilibrated with 120 mL of buffer B. Purified IRAK-4 DD was thawed in water at 25°C, and 500 μL of the solution was applied to the column. Buffer B was used at a flow rate of 1 mL/min to elute (2-mL fractions) IRAK-4 DD from the column. A 12% SDS-PAGE gel was used to analyze peak fractions.

Crystallization and Cryoprotection

A 4-mL aliquot of IRAK-4 DD was thawed in water at room temperature and subsequently placed on ice. An Amicon Ultra centrifugal filter device (Millipore, Cork, Ireland) with a 5000-Da MWCO was equilibrated with 20 mM HEPES (pH 7.5), 100 mM KCl (buffer B) at 4°C in a Sorvall H6000A swinging-bucket rotor at 3500 rpm. The thawed sample of IRAK-4 DD was exchanged into buffer B by ultra-filtration, and concentrated to a final volume of ~200 μL. The concentrated sample was placed in a 1.5-mL microcentrifuge tube and spun (16,100 RCF, 4°C, 10 min) to remove a white precipitate that formed during the final concentration step. The pelleted precipitate was discarded and the concentration of protein in the supernatant was determined by the Bradford assay (Biorad, Richmond, CA). The protein was adjusted to a final concentration of 10 mg/mL and used for crystallization screens. An initial screen using 400 different conditions from commercially available screens (Hampton Research, Aliso Viejo, CA, and Emerald Biosystems, Bainbridge Island, WA) was used to find conditions amenable to crystallization for IRAK-4 DD. All crystallization experiments were performed using the hanging-drop method of vapor diffusion. A 150-μL reservoir volume was used in 48-well VDX plates (Hampton Research). Equal volumes of the reservoir (1.2 μL) and protein (1.2 μL) solutions were mixed and suspended over a reservoir volume of 150 μL at 25°C and stored at 8°C. Well-formed crystals were observed using a reservoir solution composed of 100 mM HEPES (pH 7.5) and 25% PEG 3350. Using a home source, the diffraction from these initial crystals was poor. Various additives were screened in order to improve the diffraction limits of the crystals. The addition of $MnCl_2 \cdot 4H_2O$ (Hampton Research), to a final drop concentration of 10 mM, resulted in the formation of crystals that diffracted Cu-K_a X-rays to better than 2.5 Å. For cryoprotection, crystals were soaked for 30 min in solutions containing 100 mM HEPES (pH 7.5) and 25% PEG 3350 with 10%, 20%, and 30% increments of glycerol. Phases were determined by the multiwavelength anomalous diffraction method, utilizing crystals soaked in 30% glycerol, 100 mM HEPES (pH 7.5), 25% PEG 3350, 1 M NaBr, for 30 sec.

Data Collection

Crystals were harvested within a week of forming, mounted on 0.1- to 0.2-mm nylon loops (20-μm thickness, Hampton Research) and plunged into liquid nitrogen for storage. X-ray diffraction data from IRAK-4 DD native crystals were collected using a MAR CCD detector (120-mm distance) at 12.667 keV under standard cryogenic conditions at synchotron beamline 14-ID at Advanced Photon Source (APS), Argonne National laboratory (Argonne, IL). Diffraction data on the bromide-soaked crystals of IRAK-4 DD were collected on a MAR CCD detector (130-mm distance) at 13.480, 13.484, and 13.584 keV at synchotron beamline 32-ID at APS. The native crystal was rotated through a total of 200° with 1.0° oscillation per frame (3-sec exposures) and the bromide-soaked crystal was rotated through a total of 360° with 1.0° oscillation per frame (2-sec exposures). Initial phase-angle determination utilized the dispersive and anomalous signals from the multiwavelength anomalous diffraction data sets. Phase improvement by solvent flattening and phase extension to 1.7 Å produced a readily interpretable map. Details of the structure, including refinement statistics and PDB deposition, are reported elsewhere.[9]

RESULTS AND DISCUSSION

As part of our ongoing efforts towards the biochemical and biophysical characterization of key mediators in the innate immune pathway, we have determined the high-resolution crystal structure of the death domain

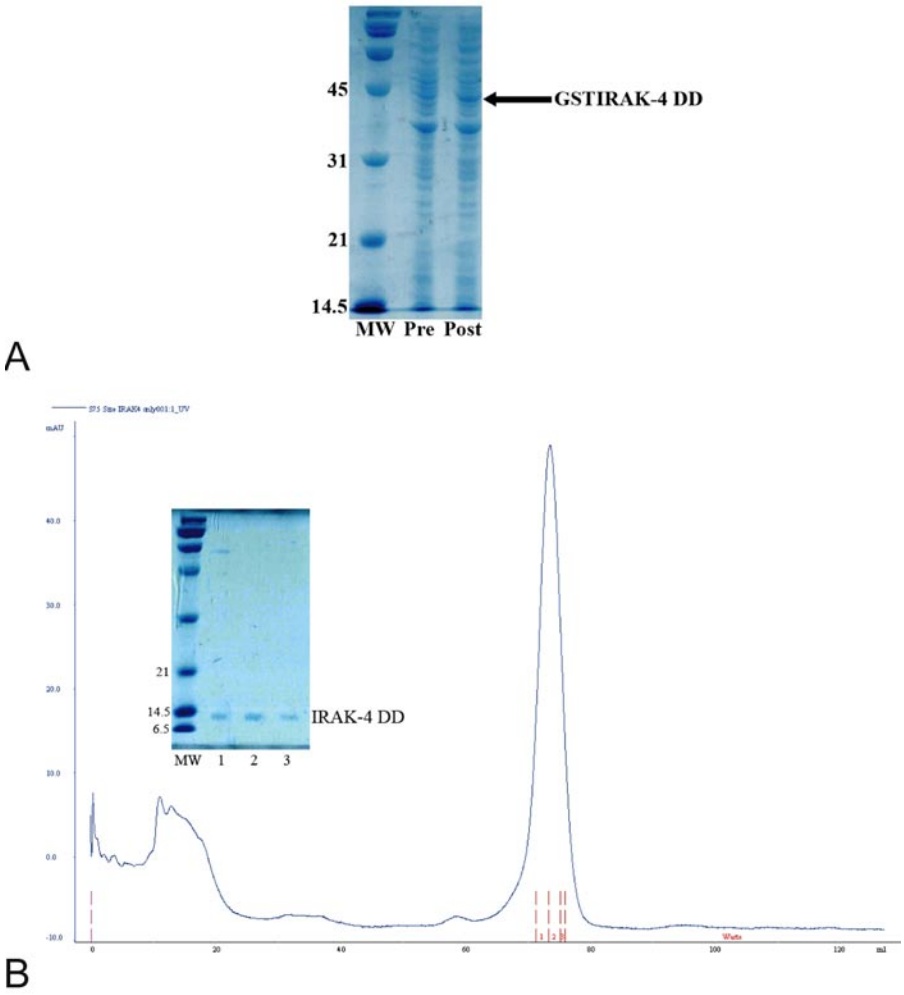

FIGURE 1

Overexpression of GSTIRAK-4 DD and the aggregation state of IRAK-4 DD. **A**: SDS-PAGE gel loaded with molecular-weight standards (MW), lysate before induction with IPTG (Pre) and after induction with IPTG (Post). Numbers designate size of standards in kilodaltons. **B**: Chromatogram of the IRAK-4 DD gel filtration elution profile and a SDS-PAGE gel loaded with corresponding fractions is inset within the chromatogram.

of IRAK-4.[9] Production of the protein as a glutathione S-transferase fusion yielded soluble samples when overexpressed in *E. coli* (Figure 1A). The use of the GST fusion also facilitated purification by affinity chromatography. Although the removal of the fusion tag slightly decreased the solubility of the IRAK-4 DD, the purified protein was not prone to further aggregation, as determined by size-exclusion chromatography (Figure 1B).

IRAK-4 DD Represents a Stable Core and Generates Well-Formed Crystals

Initial screening attempts identified well-formed crystals using polyethylene glycol 3350 as a precipitant. However, the crystals diffracted only to 4 Å using X-rays from a Cu-Kα home source (Figure 2A). Speculating that diffraction from these crystals was limited due to the presence of disordered regions within the polypeptide, the purified sample was subjected to limited proteolysis utilizing a battery of specific and non-specific proteases to identify unstructured regions. However, the purified sample was resistant to proteolysis under various conditions, suggesting that the IRAK-4 DD construct we had generated constituted a well-folded domain without any disordered regions.

Addition of Manganese (II) Improves Diffraction Dramatically

Various additives were screened in order to identify compounds that would further stabilize the crystal lattice and improve the diffraction qualities of these crystals. Addition of $MnCl_2 \cdot 4H_2O$ to a final drop concentration of 10 mM resulted in a marked improvement in the diffraction limits from these crystals (Figure 2B) with an identical crystal morphology, as observed previously. The structure was solved to 2.0-Å resolution by the multi-wavelength anomalous diffraction method, utilizing crystals transiently soaked in high concentrations of sodium bromide.[10] The structure was further refined to 1.7 Å utilizing amplitudes from a native crystal lacking halides.[9]

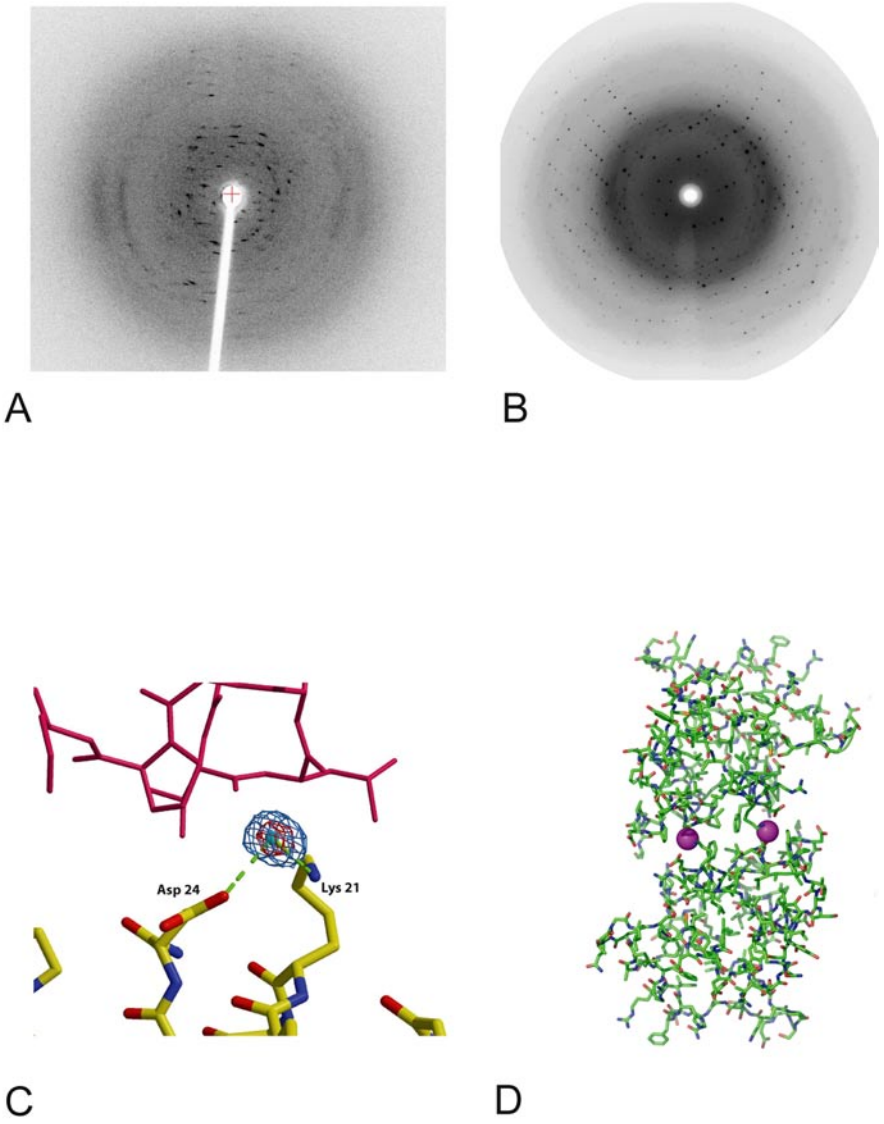

FIGURE 2

The effect of manganese (II) ions on the diffraction pattern quality and the location of the manganese ion within the structure of IRAK-4 DD. **A**: Diffraction pattern of IRAK-4 DD crystals that were grown in the absence of $MnCl_2$. **B**: Diffraction pattern of IRAK-4 DD crystals that were grown in the presence of $MnCl_2$. **C**: Ball and stick model of IRAK-4 DD where carbon, nitrogen, and oxygen atoms are denoted in yellow, blue, and red, respectively. The symmetry related molecule is represented in magenta and the manganese ion in cyan. Blue and red grids surrounding the manganese ion represent the eight and twelve sigma electron density peaks, respectively. **D**: Ball and stick model of IRAK-4 DD where carbon, nitrogen, and oxygen atoms are indicated in green, blue, and red, respectively. The manganese ion is represented as a magenta sphere. IRAK-4 DD structure coordinates have been deposited in the Protein Data Bank, PDB code 2A9I.

Manganese (II) is Coordinated to Lys-21 and Asp-24

Inspection of the 1.7-Å native structure revealed the presence of a 12 sigma peak in difference SIGMAA[11] maps calculated with model phases (Figure 2C). Based on the presence of a high concentration of manganese in the crystallization solution and the proximity of the protein ligands, a manganese ion has been assigned to this feature in the model (Figure 2C). This manganese ion is engaged by protein residues Lys-21 (distance from Nζ = 2.08 Å) and Asp-24 (distance from Oδ2 = 2.7 Å). These distances are typical of those observed for interactions with manganese in other protein structures, phosphoenolpyruvate carboxykinase (PCK) (2.3 Å average[12,13]), and arginase-I (2.2 Å average[14,15]). Lys ($pK_a = 10.53$) has been known to coordinate with manganese (II) as seen in the PCK structure.[12,13] Although a neighboring residue in the IRAK-4 DD, Arg-20 ($pK_a = 12.48$), does not coordinate with the manganese, it serves to lower the pK_a of the Lys side chain and keep it in the deprotonated state. In the deprotonated state, Lys-21 is free to coordinate to the manganese cation. Lys-21 makes a true inner-sphere coordination interaction with manganese, as the $N\zeta Mn^{+2}$ separation is 2.08 Å; however, Asp-24 makes an outer-sphere coordination with manganese.

Reduction in Surface Entropy Allows Formation of Stable Crystal Contacts

We note that metal ions are not critical for the crystallization of IRAK-4 DD, as observed in cases where such additives have been shown to be essential to crystallization.[16–20] Rather, the role of this ion is to engage the side

chains of two flexible residues that are in close proximity. Ordinarily, without manganese present, these side chains would be in numerous conformations and would not support the formation of a stable crystal contact. The reduction in conformational heterogeneity of this surface patch by the manganese coordination, generates a favorable crystal contact (Figure 2D). Reduction in conformational heterogeneity is a reduction in local surface entropy. The authors recognize that in order to lend further support to this hypothesis, structural analyses of point mutations of Lys-21 and Asp-24 to Ala residues would be helpful. However, these mutations could produce significant changes in the chemical properties of IRAK-4 DD, including changes in the stability, solubility, and aggregation state of the protein. The molecular details of the final structure have been published elsewhere.[9]

Our results with improvements in the diffraction qualities of IRAK-4 DD underscore the fact that not all well-folded, soluble, monomeric proteins yield high-quality crystals. Results from several Protein Structure Initiatives studies place the success rate for obtaining diffraction-quality crystals from well-folded, monodisperse proteins in the range of 40–50%.[21] Successful crystallization of most macromolecules requires a homogeneous sample. This requires homogeneity in both the composition and the conformation of the sample. Hence, flexible regions of macromolecules may interfere with crystal-lattice formation because of conformational heterogeneity.[22] In fact, if there is prior knowledge of the domain fold and a known region of high flexibility (i.e., a flexible loop, as in the SRβ-GTP:SRX structure[23]), one can use circular permutation as a tool to reduce surface entropy and lead to crystallization.[22]

Point Mutagenesis as a Method for Reducing Conformational Heterogeneity

In many instances, the presence of large, flexible regions in proteins can be routinely identified using limited proteolysis combined with high-resolution mass spectrometry.[24] The identified domain boundaries are used to design a new construct for the protein of interest encoding the appropriate truncations, which represent a stable core. In addition to these large regions of heterogeneity, flexible side chains, such as Lys, Arg, and Glu, can introduce conformational heterogeneity and small regions of surface flexibility. These small regions of flexibility can be problematic if they are located in a crystal contact region. In these cases, an alternative approach towards reducing conformational heterogeneity has been the use of surface-entropy reduction mutagenesis.[25,26] This approach entails the replacement of clusters of flexible side chains (i.e., Lys, Glu, and Arg) with short aliphatic residues (typically Ala) in order to induce local reduction in conformational heterogeneity.[27,28] This technique has been shown to yield improvements in diffraction, as well as facilitate *de novo* crystallization.[26,29] However, this methodology is time-consuming, as many such mutants may need to be screened in order to identify those that prove amenable to crystallization.

Reductive Methylation and Surface Entropy Reduction

Reductive methylation has been utilized as an alternate approach to surface entropy reduction.[30] Reductive methylation is thought to affect surface entropy reduction by increasing the hydrophobicity of Lys side chains, resulting in a decrease in thermal motion.[30] This technique has been successful in yielding crystals of malto-oligosyl trehalose synthase,[31] pokeweed antiviral protein,[32] Pvs25,[33] and BmBKTtx1.[34] Moreover, this technique is shown to be sufficiently gentle to facilitate the crystallization of multi-protein complexes such as the YopN-SycN-YscB ternary complex and its selenomethionine derivatives.[35]

Metal Ion–Mediated Reduction in Surface Entropy

Here we report the use of divalent metal ions, in particular manganese, as a successful alternate to the above approaches in reducing surface entropy. In the case of the IRAK-4 DD, the diffraction limits from initial crystals were presumably compromised by the presence of a cluster of flexible side chains in a loop region including Arg-20-Lys-21-X-X-Asp-24. Utilization of manganese salts as an additive resulted in a marked improvement in the diffraction limits from these crystals. Examination of the final refined structure reveals that a single manganese ion (as characterized by a 12σ peak in difference Fourier maps) engages Lys-21 and Asp-24 (Figure 2C). This results in a fixed conformation for the side chains of both residues, which would presumably be otherwise flexible, resulting in a local reduction in conformational heterogeneity of the sample. This conformationally homogenous surface patch can then form a stable crystal contact (Figure 2D). The use of manganese ions (and divalent metals in general) may be a generally applicable alternative or a suitable complement to methods such as surface entropy–reduction mutagenesis or reductive methylation towards the production of diffraction-quality crystals.

Potential of Manganese vs. Magnesium for Surface-Entropy Reduction

We note that manganese is not present in any of the commercially available crystallization screens from Hampton

Research or Emerald Biostructures, but is available only as an additive optimization reagent (Hampton Research Additive Screen 1, Condition #7). However, magnesium is present in numerous screens. Mn^{+2}, as a softer Lewis acid, has a much higher affinity for softer Lewis bases, such as amino groups, than Mg^{+2}.[13] In the case of the IRAK-4 DD, Mg^{+2} would have been able to coordinate to Asp-24 by virtue of the stronger Lewis base offered by the oxygen, but it is unlikely that Lys-21 would be able to coordinate to Mg^{+2}. The greater affinity that Mn^{+2} has for nitrogen-containing coordination environments lends itself to reducing the conformational heterogeneity of Lys residues where the utility of Mg^{+2} might be limited. Thus manganese might offer a way to easily reduce surface entropy and increase the diffraction quality of crystals or favor crystallization. Given the rapid and inexpensive nature of screening additives, the use of manganese ions may also be a valuable asset in the context of high-throughput structural genomics initiatives.

ACKNOWLEDGMENTS

We would like to thank the staff of beamlines 14-ID (K. Brister) and 32-ID (J. Brunzelle) at APS for their support. In addition, we are also grateful to D.L. Cudiamat for technical assistance and J.J. Yu and T.A. Graham for critical comments on this manuscript. This work was supported by start-up funds and the Institute for Genomic Biology, University of Illinois, Urbana-Champaign (to S.K.N.). M.V.L. was supported by an individual National Institutes of Health National Research Service Award 1 F30 NS 048779-01 from the National Institute of Neurological Disorders and Stroke.

REFERENCES

1. Flajnik MF, Du Pasquier L. Evolution of innate and adaptive immunity: Can we draw a line? *Trends Immunol* 2004;25:640–644.
2. Imler JL, Hoffmann JA. Toll and Toll-like proteins: An ancient family of receptors signaling infection. *Rev Immunogenet* 2000;2:294–304.
3. Janeway CA, Jr., Medzhitov R. Introduction: the role of innate immunity in the adaptive immune response. *Semin Immunol* 1998;10:349–350.
4. Imler JL, Hoffmann JA. Toll receptors in innate immunity. *Trends Cell Biol* 2001;11:304–311.
5. Akira S, Takeda K. Toll-like receptor signalling. *Nat Rev Immunol* 2004;4:499–511.
6. O'Neill LA, Fitzgerald KA, Bowie AG. The Toll-IL-1 receptor adaptor family grows to five members. *Trends Immunol* 2003;24:286–290.
7. Janssens S, Beyaert R. Functional diversity and regulation of different interleukin-1 receptor-associated kinase (IRAK) family members. *Mol Cell* 2003;11:293–302.
8. Wheeler TT, Hood KA. The mammalian innate immune system: potential targets for drug development. *Curr Drug Targets Immune Endocr Metabol Disord* 2005;5:237–247.
9. Lasker MV, Gajjar MM, Nair SK. Cutting edge: Molecular structure of the IL-1R-associated kinase-4 death domain and its implications for TLR signaling. *J Immunol* 2005;175:4175–4179.
10. Dauter Z, Dauter M. Entering a new phase: Using solvent halide ions in protein structure determination. *Structure (Camb)* 2001;9: R21–26.
11. Read RJ. Improved Fourier coefficients for maps using phases from partial structures with errors. *Acta Cryst* 1986;140–149.
12. Matte A, Tari LW, Goldie H, Delbaere LT. Structure and mechanism of phosphoenolpyruvate carboxykinase. *J Biol Chem* 1997;272:8105–8108.
13. Tari LW, Matte A, Goldie H, Delbaere LT. Mg^{2+}-Mn^{2+} clusters in enzyme-catalyzed phosphoryl-transfer reactions. *Nat Struct Biol* 1997;4:990–994.
14. Kanyo ZF, Scolnick LR, Ash DE, Christianson DW. Structure of a unique binuclear manganese cluster in arginase. *Nature* 1996;383:554–557.
15. Di Costanzo L, Sabio G, Mora A, Rodriguez PC, Ochoa AC, Centeno F, et al. Crystal structure of human arginase I at 1.29-Å resolution and exploration of inhibition in the immune response. *Proc Natl Acad Sci USA* 2005;102:13,058–13,063.
16. Trakhanov S, Quiocho FA. Influence of divalent cations in protein crystallization. *Protein Sci* 1995;4:1914–1919.
17. Newcomer ME, Jones TA, Aqvist J, Sundelin J, Eriksson U, Rask L, et al. The three-dimensional structure of retinol-binding protein. *EMBO J* 1984;3:1451–1454.
18. Newcomer ME, Liljas A, Eriksson U, Sundelin J, Rask L, Peterson PA. Crystallization of and preliminary X-ray data for an intracellular vitamin A-binding protein from rat liver. *J Biol Chem* 1981;256:8162–8163.
19. Newcomer ME, Liljas A, Sundelin J, Rask L, Peterson PA. Crystallization of and preliminary X-ray data for the plasma retinol-binding protein. *J Biol Chem* 1984;259:5230–5231.
20. Yao N, Trakhanov S, Quiocho FA. Refined 1.89-A structure of the histidine-binding protein complexed with histidine and its relationship with many other active transport/chemosensory proteins. *Biochemistry* 1994;33:4769–4779.
21. Chandonia JM, Brenner SE. Implications of structural genomics target selection strategies: Pfam5000, whole genome, and random approaches. *Proteins* 2005;58:166–179.
22. Schwartz TU, Walczak R, Blobel G. Circular permutation as a tool to reduce surface entropy triggers crystallization of the signal recognition particle receptor beta subunit. *Protein Sci* 2004;13:2814–2818.
23. Schwartz T, Blobel G. Structural basis for the function of the beta subunit of the eukaryotic signal recognition particle receptor. *Cell* 2003;112:793–803.
24. Cohen SL, Ferre-D'Amare AR, Burley SK, Chait BT. Probing the solution structure of the DNA-binding protein Max by a combination of proteolysis and mass spectrometry. *Protein Sci* 1995;4:1088–1099.
25. Kim AR, Dobransky T, Rylett RJ, Shilton BH. Surface-entropy reduction used in the crystallization of human choline acetyltransferase. *Acta Crystallogr D Biol Crystallogr* 2005;61:1306–1310.
26. Derewenda U, Mateja A, Devedjiev Y, Routzahn KM, Evdokimov AG, Derewenda ZS, et al. The structure of *Yersinia pestis* V-antigen, an essential virulence factor and mediator of immunity against plague. *Structure (Camb)* 2004;12:301–306.
27. Garrard SM, Longenecker KL, Lewis ME, Sheffield PJ, Derewenda ZS. Expression, purification, and crystallization of the RGS-like domain from the Rho nucleotide exchange factor, PDZ-RhoGEF, using the surface entropy reduction approach. *Protein Expr Purif* 2001;21:412–416.
28. Longenecker KL, Garrard SM, Sheffield PJ, Derewenda ZS. Protein crystallization by rational mutagenesis of surface residues: Lys to Ala mutations promote crystallization of RhoGDI. *Acta Crystallogr D Biol Crystallogr* 2001;57:679–688.
29. Longenecker KL, Lewis ME, Chikumi H, Gutkind JS, Derewenda ZS. Structure of the RGS-like domain from PDZ-RhoGEF: linking heterotrimeric g protein-coupled signaling to Rho GTPases. *Structure (Camb)* 2001;9:559–569.

30. Rayment I. Reductive alkylation of lysine residues to alter crystallization properties of proteins. *Methods Enzymol* 1997;276:171–179.
31. Kobayashi M, Kubota M, Matsuura Y. Crystallization and improvement of crystal quality for x-ray diffraction of maltooligosyl trehalose synthase by reductive methylation of lysine residues. *Acta Crystallogr D Biol Crystallogr* 1999;55 (Pt 4):931–933.
32. Kurinov IV, Mao C, Irvin JD, Uckun FM. X-ray crystallographic analysis of pokeweed antiviral protein-II after reductive methylation of lysine residues. *Biochem Biophys Res Commun* 2000;275:549–552.
33. Saxena AK, Saul A, Garboczi DN. Crystallization and preliminary X-ray analysis of the *Plasmodium vivax* sexual stage 25 kDa protein Pvs25, a transmission-blocking vaccine candidate for malaria. *Acta Crystallogr D Biol Crystallogr* 2004;60:706–708.
34. Szyk A, Lu W, Xu C, Lubkowski J. Structure of the scorpion toxin BmBKTtx1 solved from single wavelength anomalous scattering of sulfur. *J Struct Biol* 2004;145:289–294.
35. Schubot FD, Waugh DS. A pivotal role for reductive methylation in the de novo crystallization of a ternary complex composed of Yersinia pestis virulence factors YopN, SycN and YscB. *Acta Crystallogr D Biol Crystallogr* 2004;60:1981–1986.